CANCER GENOMICS & PROTEOMICS *19*: 428-444 (2022)
doi:10.21873/cgp.20330

Requirement of CLIC4 Expression in Human Colorectal Cancer Cells for Sensitivity to Growth Inhibition by Fucoxanthinol

REO YOKOYAMA[1], AYUMI KUSHIBIKI[1], SHIORI YAMADA[1], ATSUHITO KUBOTA[1], HIROYUKI KOJIMA[1,2], TOHRU OHTA[2], JUNICHI HAMADA[2,3], HAYATO MAEDA[4], MICHIHIRO MUTOH[5] and MASARU TERASAKI[1,2]

[1]*School of Pharmaceutical Sciences, Health Sciences University of Hokkaido, Hokkaido, Japan;*
[2]*Advanced Research Promotion Center, Health Sciences University of Hokkaido, Hokkaido, Japan;*
[3]*School of Nursing and Social Services, Health Sciences University of Hokkaido, Hokkaido, Japan;*
[4]*Faculty of Agriculture and Life Science, Hirosaki University, Aomori, Japan;*
[5]*Department of Molecular-Targeting Prevention, Graduate School of Medical Science, Kyoto Prefectural University of Medicine, Kyoto, Japan*

Abstract. *Background/Aim: Fucoxanthinol (FxOH), a marine carotenoid, induces apoptosis and anoikis in human colorectal cancer (CRC) DLD-1 cells via the down-regulation of chloride intracellular channel 4 (CLIC4) expression, a key molecule for apoptosis. However, whether FxOH is susceptible to CLIC4 expression and its regulatory mechanisms in human CRC cells remains unknown. We investigated the inhibitory effects of FxOH on six types of human CRC cells with CLIC4 regulation. Materials and Methods: The association between FxOH and CLIC4 was investigated using gene knockdown, overexpression, and transcriptome analyses. Results: CLIC4 expression in CRC cells was a significant factor associated with sensitivity to FxOH. CLIC4 regulates many cancer-related signals and participates in growth inhibition in FxOH-treated DLD-1 cells. Both CLIC4 knockdown and overexpression attenuated the inhibitory effects of FxOH on DLD-1 cells. Conclusion: Our findings suggest that the protein expression of CLIC4 and its regulating mechanisms play significant roles regarding cell death in human CRC cells by FxOH treatment. Further investigation by in vitro and in vivo models is needed to determine the effect of CLIC4.*

Correspondence to: Masaru Terasaki, School of Pharmaceutical Sciences and Advanced Research Promotion Center, Health Sciences University of Hokkaido, 1757 Kanazawa, Ishikari-Tobetsu, Hokkaido 061-0293, Japan. Tel: +81 133231211 ext. 3156, Fax +81 133231669, e-mail: terasaki@hoku-iryo-u.ac.jp

Key Words: Carotenoid, chloride intracellular channel 4, colorectal cancer cells, fucoxanthin, fucoxanthinol.

Colorectal cancer (CRC) is one of most prevalent cancers, with the third highest number of new cases (1.9 million per a total of 19.3 million) and second highest number of new deaths (0.9 million per a total of 10.0 million) worldwide, as estimated using the Global Cancer Observatory: CANCER TODAY 2020 database (1). The global incidence and mortality rates of CRC are expected to increase to more than 2.2 million new cases and 1.1 million deaths, respectively, by 2030 (2).

Point mutations in certain driver genes, such as adenomatous polyposis coli, Kirsten-ras (*KRAS*) and tumor protein p53 (*Tp53*), and aberrant regulations of many other genes and processes, such as signal transduction, tumor microenvironment formation, immune suppression, and gut microbiota alteration, are considered to contribute to carcinogenesis and disease progression (3-14).

The chloride intracellular channel (CLIC) protein family is a group of small globular proteins (28 kDa) comprising seven members: CLIC1, CLIC2, CLIC3, CLIC4, CLIC5A, CLIC5B, and CLIC6. They are ubiquitously expressed in various tissues and involved in intracellular trafficking, membrane remodeling, and other homeostatic mechanisms (15). Among these, CLIC4 has been well-studied for its association with cancer development. CLIC4 is a key molecule for apoptosis, angiogenesis, cell adhesion, wound healing, and tumorigenesis (14-20). In addition, CLIC4 expression is regulated by *KRAS* and *Tp53* (21,22). We recently revealed that the number of CLIC4 high-expressing cells tended to decrease with the progression of pathological grades in colorectal malignant tissues of patients with CRC (23). These findings were also consistent with those of a previous study (24). Moreover, high expression levels of CLIC4 protein are suggested to be correlated with poor prognosis in patients with CRC and the aggressive potential of CRC stem-like cells (25). However, the role of CLIC4 in CRC development remains unknown.

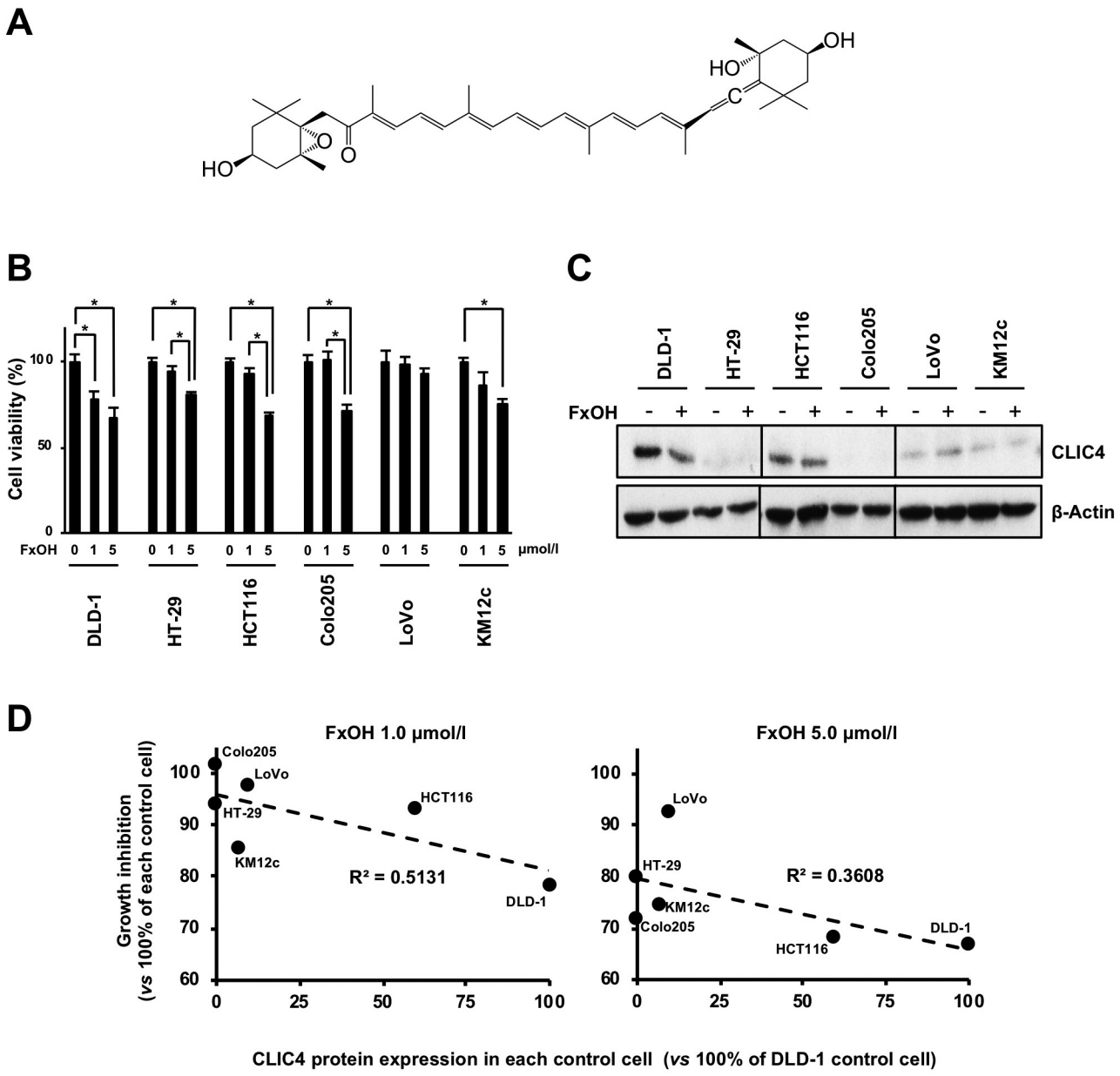

Figure 1. *Continued*

A dominant marine pigment of fucoxanthin (Fx), a non-provitamin A carotenoid, is an essential photosynthetic lipid for brown algae and microalgae (26). Humans can also obtain Fx *via* edible brown algae, such as *Undaria pinnatifida* (wakame) and *Himanthalia elongata* (sea spaghetti). Toxicological studies have revealed that Fx is a safe compound with little side effects in humans and rodents (27-29). Dietary Fx is metabolically converted to *cis*-Fx and fucoxanthinol (FxOH; Figure 1A) in the intestine, and subsequently to amarouciaxanthin A (Amx A) and *cis*-Amx A in the liver in both humans and mice. FxOH and *cis*-FxOH are the main plasma metabolites in humans when ingested with brown algae or its extract (30-32). No clinical and epidemiological data are available regarding the anticancer effects of Fx. However, anti-cancer potentials for Fx and FxOH have been well elucidated *in vivo* and *in vitro* (33-37).

Recently, we showed that FxOH treatment can induce apoptosis in human CRC DLD-1 cells *via* the suppression of CLIC4 signals comprised of CLIC4, integrin β1, Na^+/H^+ exchanger regulatory factor 2 (NHERF2), and phosphorylated Smad2, which are all significant regulators of CRC development (38-42). Interestingly, CLIC4 knockdown

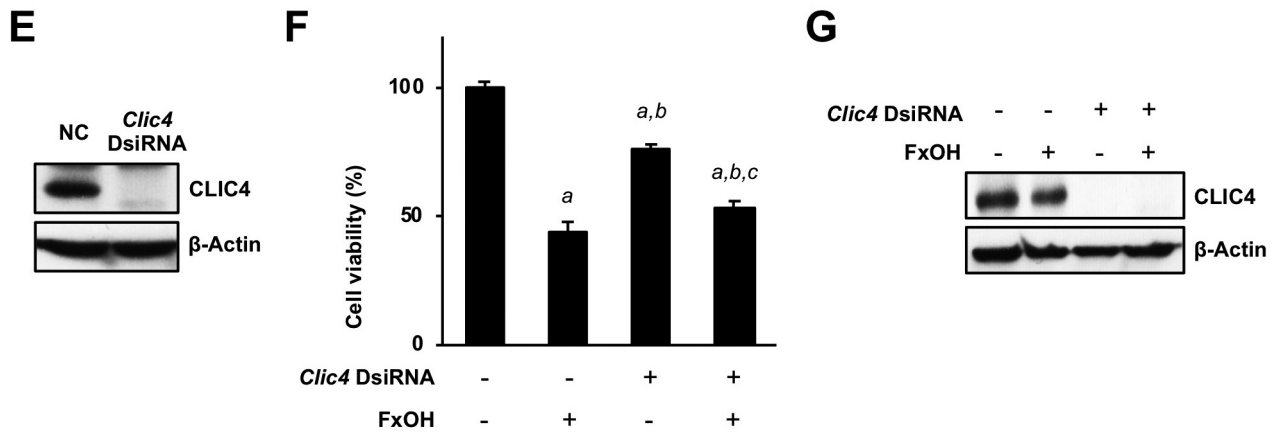

Figure 1. *Effects of FxOH on cell growth and CLIC4 expression in six of human colorectal cancer (CRC) cells, and on cell growth in DLD-1 cells with CLIC4 knockdown. (A) Fucoxanthinol (FxOH) structure. Molecular weight, 616.87 g/mol (C40H56O5). (B) Six of human CRC cells, DLD-1, HT-29, HCT116, Colo205, LoVo, and KM12C, were treated with FxOH (1.0 and 5.0 μM) for 2 days. Cell viability was determined using a tetrazolium salt [2-(4-iodophenyl)-3-(4-nitrophenyl)-5-(2,4-disulfophenyl)-2H-tetrazolium] (WST-1) assay. Mean±SE (n=6). *p<0.05. (C) CLIC4 protein levels in six human colorectal cancer cells treated with FxOH (5.0 μM) for 1 day were measured by western blotting. (D) The correlation plots between growth inhibition and CLIC4 expression in human CRC cells treated with FxOH. X-axis, CLIC4 expression in each type of control cell that was set as 100% on the CLIC4 expression of control DLD-1 cells; Y-axis, the ratio of growth inhibitions in six of CRC cells treated with FxOH (1.0 and 5.0 μM) as shown in Figure 1A. (E) DLD-1 cells were treated with Clic4 dsiRNA for 2 days. The CLIC4 protein level was measured by western blotting. NC, negative control. (F) The CLIC4 knockdown DLD-1 cells were treated with FxOH (5.0 μM) for 1 day. The cell viability was assessed by a WST-1 assay. Mean±SE (n=6). a, *p<0.05 vs. negative control cells with vehicle alone; b, *p<0.05 vs. negative control cells with FxOH; c, *p<0.05 vs. CLIC4 knockdown cells with vehicle alone. (G) CLIC4 protein levels in negative control and CLIC4 knockdown in DLD-1 cells with and without FxOH treatment were measured by western blotting, respectively.*

attenuated the apoptotic potential of FxOH in cells (38). Moreover, alterations in cancer-related signals, such as the cell cycle, adhesion, and phosphoinositide 3-kinase (PI3K)/serine-threonine kinase protein B (AKT) expression, and the induction of anchor-dependent cell detachment (anoikis) were observed in FxOH-treated DLD-1 cells (38, 43-45). These findings led us to assume that sensitivity to apoptosis and anoikis induction by FxOH in human CRC cells may depend on the protein expression levels of CLIC4 and its regulatory mechanisms. However, the detailed mechanism remains unclear.

In the present study, we investigated the growth inhibitory effect of FxOH *via* CLIC4 regulation in human CRC cells and elucidated its underlying molecular mechanisms.

Materials and Methods

Chemicals. All-*trans*-FxOH (purity ≥ 98%) was kindly donated by Dr. Hayato Maeda (Hirosaki University, Japan) (Figure 1). Dulbecco's modified Eagle's medium (DMEM) and fetal bovine serum (FBS) were purchased from FUJIFILM Wako Pure Chemicals (Osaka, Japan). Human CRC cells (DLD-1, HT-29, HCT116, Colo205, LoVo, and KM12C) were obtained from the American Type Culture Collection (Rockville, MD, USA). The cells were maintained in DMEM supplemented with 10% heat-inactivated FBS, L-glutamine (4 mM), penicillin (40,000 U/l), and streptomycin (40 mg/L). Lipofectamine RNAiMAX, Lipofectamine 3000, Opti-MEM I, RNAlater, penicillin/streptomycin, and GlutaMAX were obtained from Thermo Fisher Scientific (Carlsbad, CA, USA). DynaMarker RNA high for easy electrophoresis was obtained from the BioDynamics Laboratory (Tokyo, Japan). Anti-β-actin, anti-CLIC4, and anti-interferon induced protein with tetratricopeptide repeats 1 (IFIT1) antibodies were obtained from GeneTex (Irvine, CA). Anti-claudin-2 (CLDN2) and anti-c-KIT antibodies were purchased from Novus Biologicals (Littleton, CO, USA) and R&D Systems (Minneapolis, MN, USA), respectively. The premixed water-soluble tetrozolium (WST)-1 cell proliferation assay system was obtained from Takara Bio (Shiga, Japan). All other reagents and solvents used in this study were of high grade.

Cell viability. DLD-1, HT-29, HCT116, Colo205, LoVo, and KM12C cells were seeded at a density of 5×10^4 cells/ml in a 24-well plate in 10% FBS/DMEM. After adherence for 3.5 h, the medium was replaced with fresh 1% FBS/DMEM medium containing FxOH (final concentration, 1.0 and 5.0 μmol/l) or vehicle (dimethyl sulfoxide, DMSO) and incubated for 1 day. Cell viability was evaluated using a WST-1 assay and measured at 450 nm wavelength using an enzyme-linked immunosorbent assay reader (TECAN Japan, Tokyo, Japan).

CLIC4 knockdown and overexpression. Two 27-mer dicer-substrate short interfering RNAs (dsiRNAs) encoding *CLIC4* mRNA in *Homo sapiens* were synthesized by Integrated DNA Technologies (Coralville, IA, USA). The *CLIC4* dsiRNAs used were as follows: dsiRNA-1, 5'-GCUCUCUAUUCUAGUUGAUAAAACT-3' and dsiRNA-2, 5'-CAAAUUCUCUGCAUAUAUCAAGAAT-3'. A dsiRNA sequence of the negative control (NC), 5'-GUGUUCU

ACACCAUUACUCAAUUCUUA-3', was prepared for CLIC4 knockdown. A CLIC4 ORF plasmid cDNA (pcDNA) 3.1(+)-CMV mammalian expression vector (Clone, OHu22609D) was constructed for CLIC4 overexpression using GenScript (Piscataway, NJ, USA). Lipofectamine RNAiMAX and Opti-MEM I reduced serum medium were used to prepare dsiRNA complexes, according to the manufacturer's instructions. For CLIC4 knockdown, 5.5 μl of dsiRNA or NC was added to 30 μl of Lipofectamine RNAiMAX and mixed with 1,000 μl of Opti-MEM I medium. DLD-1 cells were seeded in 100-mm dishes at a density of 8×10^4 cells/ml and allowed to adhere for 1 d for both CLIC4 knockdown and overexpression. The dsiRNA -1, -2, or NC complex was then added to 10 ml of 10% FBS/DMEM (final concentration of dsiRNA, 10 nmol/l) for 1 day. The medium was then changed to 10% FBS/DMEM containing the new dsiRNA complex for 1 day.

Lipofectamine 3000 and Opti-MEM I reduced-serum medium were used to prepare pcDNA complexes, according to the manufacturer's instructions. For CLIC4 overexpression, 4 μg of pcDNA solution or vehicle (Tris-ethylenediaminetetraacetic acid, TE buffer) was mixed with 200 μl of Opti-MEM I reduced-serum medium (mixture-A). Subsequently, Lipofectamine 3000 was mixed with 200 μl of Opti-MEM I reduced-serum medium at room temperature for 5 min (mixture-B). Mixtures A and B were mixed at room temperature for 20 min, added to 10 ml of cell culture medium (final concentration of pcDNA, 0.4 μg/ml), and incubated at 37˚C for 1 day. The medium was then changed to 10% FBS/DMEM containing the new pcDNA complex for 1 day.

Cells with or without CLIC4 knockdown and overexpression were seeded at a density of 5×10^4 cells/ml in a 24-well plate in 10% FBS/DMEM. After adherence for 3.5 h, the cells were reintroduced into the medium containing FxOH (final concentration, 5 μmol/l) or vehicle (DMSO) in 1% FBS/DMEM and incubated for 1 day. Cell growth was measured using a tetrazolium salt [2-(4-iodophenyl)-3-(4-nitrophenyl)-5-(2,4-disulfophenyl)-2H-tetrazolium] (WST-1) cell viability assay.

Total RNA extraction and purification. Total RNA was extracted from each whole cell and purified using the RNeasy Mini Kit and RNase-Free DNase Set (QIAGEN, Valencia, CA, USA), according to the manufacturer's instructions. The concentration of total RNA was determined using Nanodrop ND-1000 (NanoDrop, Wilmington, DE, USA). Total RNA was quantified using 1.3% agarose gel electrophoresis based on 18S and 28S rRNAs and DynaMarker RNA High for Easy Electrophoresis.

Transcriptome analysis. Transcriptome analysis of each whole cell was performed using a Clariom™ S human assay (GeneChip) with the standard enzymes and reagents kit (Thermo Fisher Scientific, Carlsbad, CA, USA). First, 50 ng of total RNA was mixed with the poly(A)-RNA controls. First-strand cDNA was enzymatically generated from RNA templates and second-strand cDNA was subsequently synthesized. *In vitro* transcription using T7 RNA polymerase was conducted for the massive preparation of single-stranded cRNA from double-stranded cDNA. The resulting single-stranded cRNA (15 μg) was purified using a magnetic purification bead and converted into second-cycle single-stranded cDNA. The cDNA template was then purified using a magnetic purification bead, fragmented by uracil-DNA glycosylase and apurinic/apyrimidinic endonuclease 1, and biotin-labeled with terminal deoxynucleotidyl transferase. The labeled cDNA (2.3 μg) was then hybridized to GeneChip, washed, and stained using Affymetrix Fluidics Station 450 with stain solutions (Affymetrix, Santa Clara, CA, USA). GeneChip was scanned using the Affymetrix GeneChip Scanner 3000 system (Affymetrix). Data were analyzed using Transcriptome Analysis Console (TAC) software version 4.0.2 (Applied Biosystems, Foster City, CA, USA). The genes with significant differences between the two groups were evaluated using ≥2.0 and ≤–2.0-fold with cutoff *p*-value [one-way analysis of variance (ANOVA), $p<0.05$]. Principal coordinate analysis (PCoA), volcano plots, hierarchy clustering, and wikipathways were performed using the TAC software.

Western blotting analysis. Cells were collected and lysed using the lysis buffer. Protein concentration was determined using the Bradford assay (Bio-Rad, Hercules, CA, USA). Ten micrograms of whole cell lysate were subjected to sodium dodecyl sulfate-10% polyacrylamide gel electrophoresis and then electroblotted onto a polyvinylidene difluoride (PVDF) membrane (Amersham Bioscience, Little Chalfont, UK). The PVDF membrane was washed with Tris-buffered saline containing 0.1% Tween 20 (TBS-T) and blocked with 1% w/v bovine serum albumin (BSA) in TBS-T (1% BSA/TBS-T) at room temperature for 1 h. Subsequently, the membrane was incubated with each primary antibody (diluted 1:1,000) in 1% BSA/TBS-T at 4˚C overnight. The membrane was washed with TBS-T and incubated with horseradish peroxidase-conjugated anti-mouse or anti-rabbit secondary antibodies in 1% BSA/TBS-T at room temperature for 1 h. Protein bands in the membrane were observed using a chemiluminescence assay (Millipore, Billerica, MA, USA).

Statistical analysis. All values are represented as the mean±standard error. Statistical analysis was performed using one-way ANOVA with Tukey–Kramer *post hoc* tests for multiple comparisons. Differences were considered to be statistically significant at $*p<0.05$ and exact *p*-Values were calculated by an exact test on edge R in the TAC software.

Results

Effect of FxOH on the growth of human CRC cells. The effect of FxOH on the growth of six human CRC cells was determined. The growth of DLD-1, HT-29, HCT116, Colo205, and KM12C cells was significantly inhibited by FxOH treatment in a dose-dependent manner. However, little significant difference in LoVo cell growth was observed (Figure 1B). In addition, FxOH treatment clearly decreased CLIC4 protein expression levels in DLD-1 and HCT116 cells, but not in HT-29, Colo205, LoVo, and KM12C cells (Figure 1C). An inverse correlation was found between the growth inhibitory level of each cell with FxOH treatment and CLIC4 expression level in each control cell (100% in that of DLD-1 control cell): R^2 values in FxOH 1.0 and 5.0 μmol/l were 0.5131 and 0.3608, respectively (Figure 1D). DLD-1 cells treated with DsiRNA for two days showed decreased CLIC4 protein expression compared to NC cells (Figure 1E). CLIC4 knockdown and NC cells were collected, seeded onto a culture plate, and treated with FxOH (5.0 μmol/l). Cell growth in CLIC4 knockdown control cells was significantly

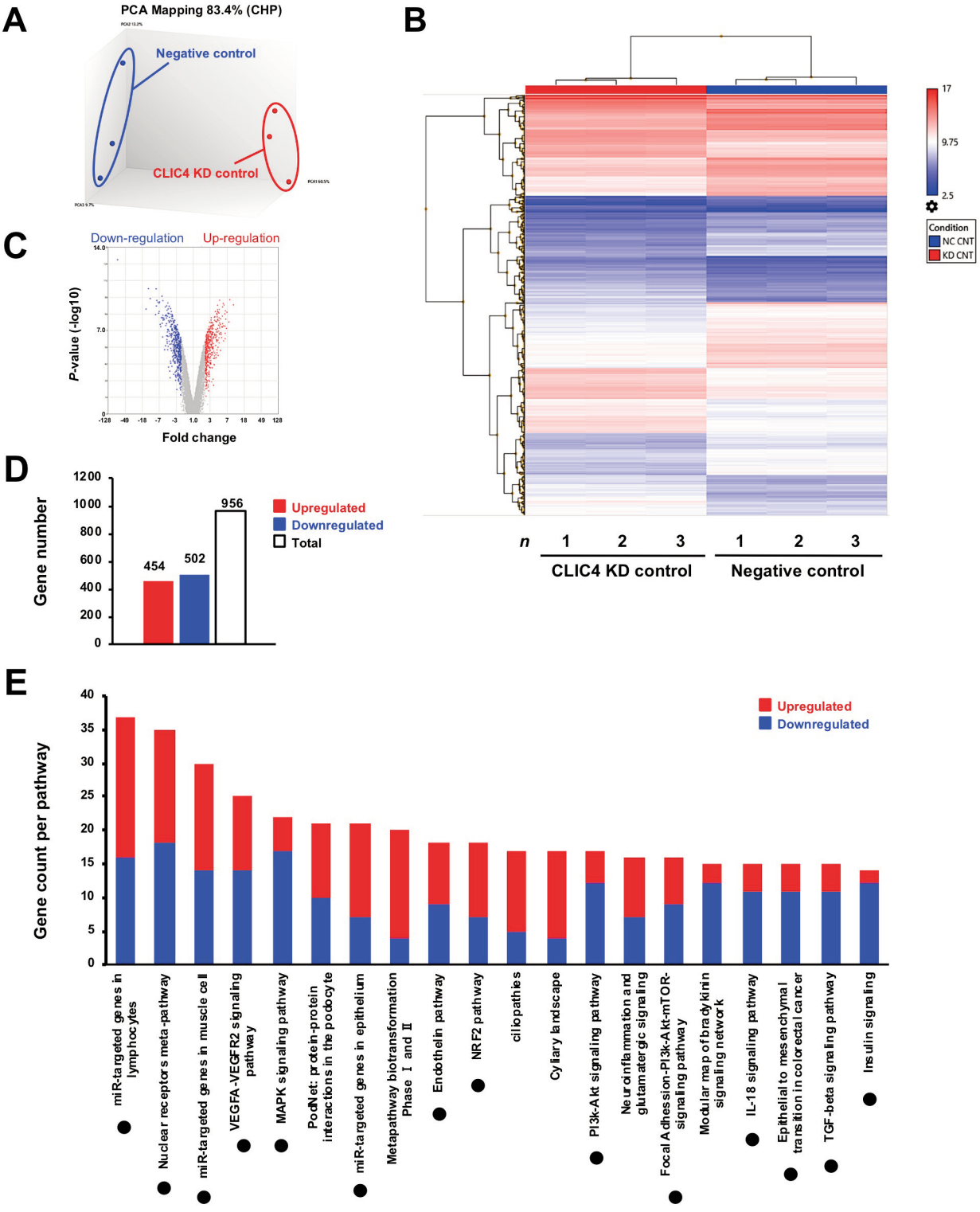

Figure 2. *Gene expression profiles in DLD-1 cells with or without CLIC4 knockdown. Gene expression levels between the CLIC4 knockdown (KD) DLD-1 cells (group 1) and the negative control cells (group 2) were subjected to Clariom™ S human assays and TAC software (n=3). (A) PCoA plot indicating genetic differences among different samples. (B) Hierarchical cluster analysis for 956 genes between groups 1 and 2. (C) Volcano plots between groups 1 and 2. (D) Number of up- (≥2.0-fold) and down-regulated (≤–2.0-fold) genes between groups 1 and 2. (E) The distribution of the top 20 gene sets that changed between group 1 and 2. Black circles indicate the gene set involving cancer development. The p-Value was determined using two-sided Fisher's exact test. The value implies an index measuring bias of the gene set in DLD-1 cells with CLIC4 knockdown.*

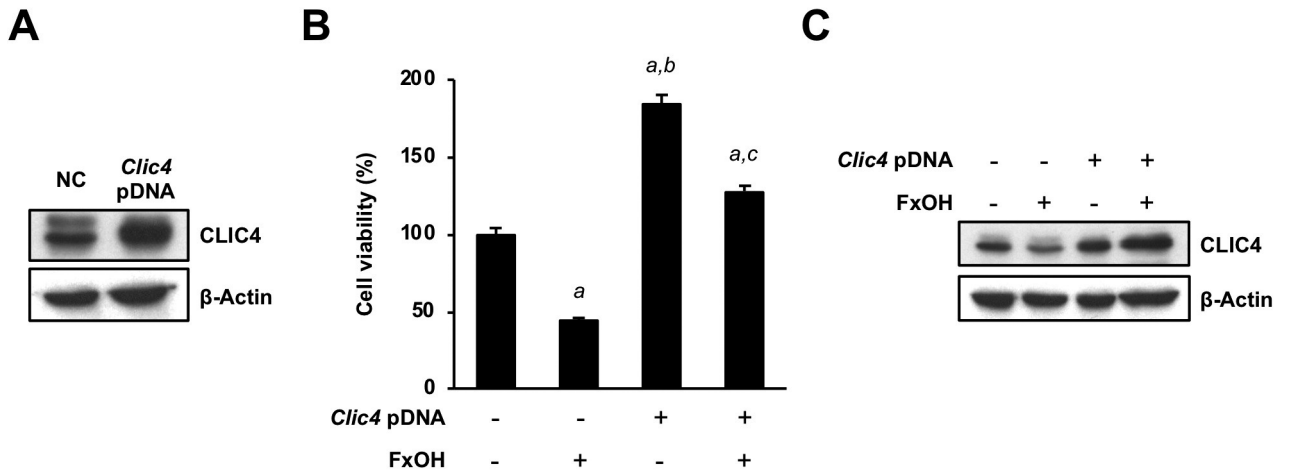

Figure 3. *Effects of FxOH on cell growth and CLIC4 expression in DLD-1 cells with CLIC4 overexpression. DLD-1 cells were treated with Clic4 plasmid DNA [(p)DNA] for 2 days. (A) The CLIC4 protein level was measured by western blotting. NC, negative control. (B, C) The CLIC4 overexpression DLD-1 cells were treated with FxOH (5.0 μM) for 1 day. (B) Cell viability was assessed by a tetrazolium salt [2-(4-iodophenyl)-3-(4-nitrophenyl)-5-(2,4-disulfophenyl)-2H-tetrazolium] (WST-1) assay. Mean±SE (n=6-10). a, *p<0.05 vs. negative control cells with vehicle alone; b, *p<0.05 vs. negative control cells with FxOH; c, *p<0.05 vs. CLIC4 overexpression cells with vehicle alone. (C) CLIC4 protein levels in negative control and CLIC4 overexpression DLD-1 cells with and without FxOH treatment were measured by western blotting, respectively.*

decreased compared with that in NC control cells. The inhibitory effect of FxOH on cell growth in CLIC4 knockdown cells with FxOH was significantly attenuated compared to that of the cell growth in NC cells with FxOH (Figure 1F). The protein expression levels of CLIC4 were decreased in NC cells with FxOH treatment, whereas those in CLIC4 knockdown DLD-1 cells were not detected with or without FxOH treatment (Figure 1G).

Transcriptome alterations in human CRC DLD-1 cells following CLIC4 knockdown. First, the transcriptome changes in CLIC4 knockdown DLD-1 cells were determined. The PCoA plot showed major genetic differences between CLIC4 knockdown and NC cells (Figure 2A). Hierarchical clustering of 956 genes revealed large differences between CLIC4 knockdown and NC DLD-1 cells (Figure 2B). The volcano plot revealed that the levels of both gene fold differences and *p*-values on the down-regulated genes in CLIC4 knockdown control cells were higher than those in the NC cells (Figure 2C). Overall, 454 up-regulated and 502 down-regulated genes (a total of 956 genes) were obtained in CLIC4 knockdown control cells compared to NC cells (Figure 2D). Pathway analysis showed that 14 of the top 20 gene sets, namely nuclear receptor (NR), vascular endothelial growth factor (VEGF), mitogen-activated protein kinase (MAPK), endothelin, nuclear factor-erythroid 2-related factor 2 (NRF2), PI3K/AKT, adhesion, interleukin (IL)-18, epithelial–mesenchymal transition (EMT), transforming growth factor (TGF)-β, and insulin signaling, were involved in gene groups for cancer development, including three types of microRNA (miRNA) regulation (Figure 2E, black circle).

Effect of FxOH on the growth of CLIC4-overexpressing human CRC DLD-1 cells. The effect of FxOH on the growth of CLIC4-overexpressing DLD-1 cells was also determined. DLD-1 cells treated with CLIC4 pDNA for two days showed increased CLIC4 protein expression levels compared to NC cells (Figure 3A). The CLIC4 overexpression and NC cells were collected, seeded onto a culture plate, and treated with FxOH (5.0 μmol/l). Cell growth in CLIC4 overexpression control cells was significantly increased compared with that in NC control cells. The inhibitory effect of FxOH on cell growth in CLIC4 overexpression cells was significantly attenuated compared to that of the cell growth in NC cells (Figure 3B). The protein expression levels of CLIC4 decreased in NC cells with FxOH treatment, whereas those in CLIC4 overexpression cells with FxOH treatment did not change either with or without FxOH treatment (Figure 3C).

Transcriptome alterations in CLIC4-overexpressing human CRC DLD-1 cells. Transcriptomic changes in the CLIC4-overexpressing DLD-1 cells were determined. The PCoA plot showed major genetic differences between CLIC4 overexpression and NC cells (Figure 4A). Hierarchical clustering of 69 genes showed large differences between CLIC4 overexpression and NC cells (Figure 4B). The volcano plot revealed that the levels of both gene fold differences and *p*-values on the up-regulated genes in CLIC4

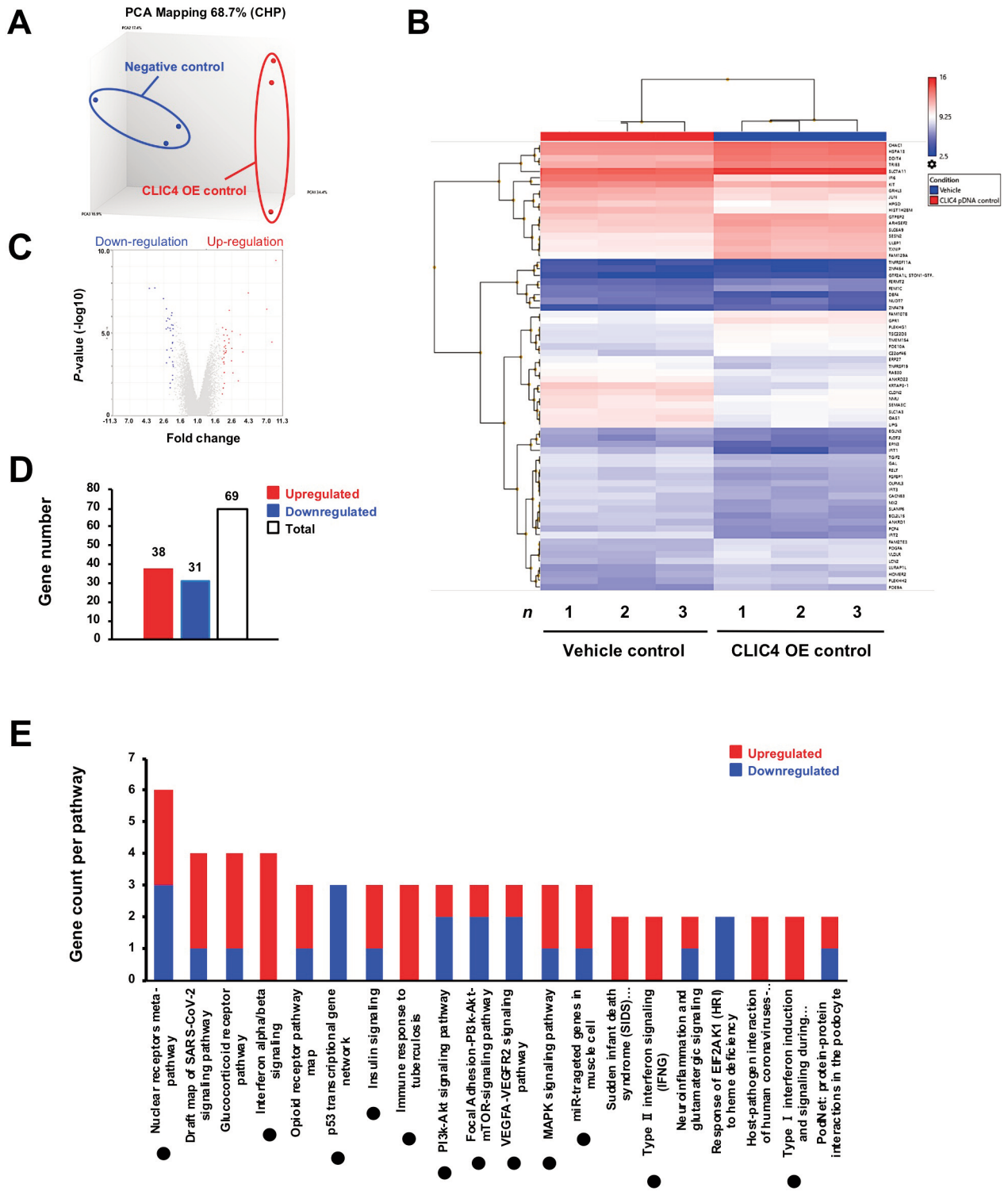

Figure 4. *Gene expression profiles in DLD-1 cells with or without CLIC4 overexpression. Gene expression levels between the CLIC4 overexpression (OE) DLD-1 cells (group 1) and the negative control cells (group 2) were subjected to Clariom™ S human assays and TAC software (n=3). (A) PCoA plot indicating genetic differences among different samples. (B) Hierarchical cluster analysis for 69 genes between groups 1 and 2. (C) Volcano plots between groups 1 and 2. (D) Number of up- (≥2.0-fold) and down-regulated (≤–2.0-fold) genes between groups 1 and 2. (E) The distribution of the top 20 gene sets that changed between group 1 and 2. Black circles indicate the gene set involving cancer development. The p-Value was determined using two-sided Fisher's exact test. The value implies an index measuring bias of the gene set in DLD-1 cells with CLIC4 knockdown.*

Table I. *Up-regulated gene profile in DLD-1 cells with CLIC4 knockdown*[a].

Gene symbol	Description	Fold[b]	*p*-Value[c]
Group 1[d]			
CLDN2	Claudin 2	6.24	4.73×10^{-7}
ERP27	Endoplasmic reticulum protein 27	6.19	4.16×10^{-8}
IFIT1	Interferon-induced protein with tetratricopeptide repeats 1	2.84	1.77×10^{-6}
FGFBP1	Fibroblast growth factor binding protein 1	2.76	6.52×10^{-5}
SLC1A3	Solute carrier family 1, member 3	2.46	1.69×10^{-5}
LIPG	Lipase, endothelial	2.04	1.20×10^{-3}
Group 2[e]			
FERMT2	Fermitin family member 2	2.64	1.33×10^{-5}
GPR1	G protein-coupled receptor 1	2.19	0.0008
VLDLR	Very low density lipoprotein receptor	2.13	3.13×10^{-3}
Group 3[f]			
PSAT1	Phosphoserine aminotransferase 1	9.93	6.76×10^{-10}
NEK7	NIMA-related kinase 7	8.12	2.53×10^{-10}
SCEL	Sciellin	7.67	1.88×10^{-8}
F3	Coagulation factor III (thromboplastin, tissue factor)	6.90	2.84×10^{-9}
HMOX1	Heme oxygenase 1	6.72	6.51×10^{-8}
FAM3B	Family with sequence similarity 3, member B	6.46	1.10×10^{-8}
HINT3	Histidine triad nucleotide binding protein 3	6.27	2.12×10^{-9}
QPRT	Quinolinate phosphoribosyltransferase	6.19	1.66×10^{-7}
POLR3G	Polymerase (RNA) III (DNA directed) polypeptide G (32kD)	6.14	4.34×10^{-8}
ALPP	Alkaline phosphatase, placental	6.08	3.91×10^{-9}
ZNF770	Zinc finger protein 770	5.84	7.05×10^{-10}
LIX1L	Limb and CNS expressed 1 like	5.64	7.12×10^{-7}
FUBP3	Far upstream element (FUSE) binding protein 3	5.64	3.81×10^{-8}
SAMD15	Sterile alpha motif domain containing 15	5.53	5.19×10^{-10}
IQGAP2	IQ motif containing GTPase activating protein 2	5.42	4.77×10^{-8}
CBX1	Chromobox homolog 1	5.37	1.02×10^{-9}
UBE3C	Ubiquitin protein ligase E3C	5.33	2.54×10^{-8}
DPP4	Dipeptidyl-peptidase 4	5.30	5.98×10^{-9}
LGR5	Leucine-rich repeat containing G protein-coupled receptor 5	5.19	4.99×10^{-8}
C1orf105	Chromosome 1 open reading frame 105	5.10	4.85×10^{-8}
SLITRK6	SLIT and NTRK-like family, member 6	5.07	3.78×10^{-7}
TPRG1	Tumor protein p63 regulated 1	4.96	1.97×10^{-7}
REG4	Regenerating islet-derived family, member 4	4.86	1.45×10^{-7}
TMEM254	Transmembrane protein 254	4.81	4.52×10^{-6}
SC5D	Sterol-C5-desaturase	4.77	1.00×10^{-8}
TCTN2	Tectonic family member 2	4.67	2.90×10^{-8}
NR4A3	Nuclear receptor subfamily 4, group A, member 3	4.56	2.00×10^{-7}
MAPRE1	Microtubule-associated protein, RP/EB family, member 1	4.55	2.76×10^{-10}
HLTF	Helicase-like transcription factor	4.54	5.98×10^{-8}
ACER2	Alkaline ceramidase 2	4.53	2.26×10^{-8}
SGPP1	Sphingosine-1-phosphate phosphatase 1	4.52	4.14×10^{-8}
PGAM1	Homo sapiens phosphoglycerate mutase 1	4.46	1.69×10^{-7}
ARL6IP1	ADP-ribosylation factor like GTPase 6 interacting protein 1	4.45	1.67×10^{-9}
DAB2	Dab, mitogen-responsive phosphoprotein, homolog 2	4.41	1.06×10^{-6}
MMP15	Matrix metallopeptidase 15 (membrane-inserted)	4.39	8.54×10^{-9}
ANXA6	Annexin A6	4.36	3.96×10^{-7}
PIP5K1B	Phosphatidylinositol-4-phosphate 5-kinase, type I, beta	4.35	1.49×10^{-8}
EFR3A	EFR3 homolog A	4.32	3.34×10^{-9}
PRSS2	Protease, serine, 2 (trypsin 2)	4.27	1.06×10^{-7}
ACPP	Acid phosphatase, prostate	4.25	3.48×10^{-8}
GPR157	G protein-coupled receptor 157	4.20	2.73×10^{-9}
INSL4	Insulin-like 4 (placenta)	4.18	1.19×10^{-5}
VGLL1	Vestigial-like family member 1	4.13	2.51×10^{-6}
RRAGD	Ras-related GTP binding D	4.11	6.22×10^{-7}

Table I. *Continued*

Table I. *Continued*

Gene symbol	Description	Fold[b]	*p*-Value[c]
UGT1A1	UDP glucuronosyltransferase 1 family, polypeptide A1	4.06	1.11×10^{-8}
ABCG2	ATP binding cassette subfamily G member 2	4.04	1.73×10^{-9}
RSL24D1	Ribosomal L24 domain containing 1	4.04	1.32×10^{-8}
TNS4	Tensin 4	4.04	6.50×10^{-8}
RNF7	Ring finger protein 7	4.04	7.21×10^{-10}
RAB8B	RAB8B, member RAS oncogene family	4.04	2.57×10^{-9}
SERPINB5	Serpin peptidase inhibitor, clade B (ovalbumin), member 5	4.02	1.29×10^{-7}

[a]Among all 453 up-regulated genes with significant alterations, the 53 genes with ≥4.0-fold and 7 genes with <4.0- and ≥2.0-fold are shown. [b]Fold change of gene expression in DLD-1 cells with CLIC4 knockdown, compared with that of control cells. [c]Significant differences between DLD-1 cells with and without CLIC4 knockdown using one-way ANOVA (n=3). [d]Group 1, genes up-regulated in both CLIC4 knockdown and overexpression in DLD-1 cells, corresponding to those of group 1 in Table III. [e]Group 2, genes up-regulated in CLIC4 knockdown and down-regulated in CLIC4 overexpression, corresponding to those of group 2 in Table IV. [f]Group 3, genes up-regulated in CLIC4 knockdown but not detected in CLIC4 overexpression.

overexpression control cells were higher than those in the NC cells (Figure 4C). Overall, 38 up-regulated and 31 down-regulated genes (a total of 69 genes) were obtained in CLIC4-overexpressing control cells compared to NC cells (Figure 4D). Pathway analysis showed that 12 of the top 20 gene sets, namely NR, interferon-α, p53 transcription, insulin, immune response, PI3K/AKT, adhesion, VEGF, MAPK, microRNA regulation, and type I- and II- interferon signals, were involved in gene groups for cancer development (Figure 4E, black circle).

Expression levels of two proteins up-regulated in both CLIC4 knockdown and -overexpressing DLD-1 cells. Table I, Table II, Table III, and Table IV show the significantly altered genes in DLD-1 cells with CLIC4 knockdown and overexpression in comparison with each negative control. Six genes (≥2.0-fold), *CLDN2*, endoplasmic reticulum protein 27 (*ERP27*), *IFIT1*, fibroblast growth factor binding protein 1 (*FGFBP1*), solute carrier family 1 member 3 (*SLC1A3*), and lipase G (*LIPG*), were identified as genes up-regulated in cells with both CLIC4 knockdown and overexpression (Table I and Table III). Three genes, FERM domain containing kindlin 2 (*FERMT2*), G protein-coupled receptor 1 (*GPR1*), and very low-density lipoprotein receptor (*VLDLR*), were identified as the genes up-regulated in CLIC4 knockdown and down-regulated in CLIC4-overexpressing cells (Table I and Table IV). Four genes, TSC22 domain family member 3 (*TSC22D3*), chromosome 22 putative open reading frame 46 (*C22orf46*), transmembrane protein 154 (*TMEM154*), and leucine rich adaptor protein 1 like (*LURAP1L*), were identified as the genes down-regulated in cells with both CLIC4 knockdown and overexpression (Table II and Table IV). Nine genes, keratin associated protein 3-1 (*KRTAP3-1*), *IFIT2*, 2'-5'-oligoadenylate synthetase 1 (*OAS1*), TNF receptor superfamily member 19 (*TNFRSF19*), ankyrin repeat domain 13C (*ANKRD13C*), Purkinje cell protein 4 (*PCP4*), *JUN*, calcium voltage-gated channel auxiliary subunit beta 3 (*CACNB3*), and semaphorin 3C (*SEMA3C*), were identified as the genes down-regulated in CLIC4 knockdown and up-regulated in CLIC4-overexpressing cells (Table II and Table III). Based on these transcriptome alterations, the protein expression levels of IFIT1 and CLDN2 were determined in DLD-1 cells with CLIC4 knockdown and overexpression. The protein expression levels of CLDN2 increased in both CLIC4 knockdown and overexpressing cells. CLIC4 overexpression in cells increased IFIT1 protein expression but was not detected in CLIC4 knockdown and NC cells (Figure 5).

Discussion

The present study demonstrated that FxOH most strongly suppressed the growth of DLD-1 cells with the highest expression of CLIC4 compared to the other five types of human CRC cells. Both CLIC4 knockdown and overexpression modulated the growth of DLD-1 cells by altering many signal transduction pathways. Unexpectedly, both CLIC4 knockdown and overexpression reduced the sensitivity of DLD-1 cells to FxOH. This is the first report suggesting the significance of the protein expression of CLIC4 and its regulating mechanisms in human CRC cells for the sensitivity to FxOH.

First, we confirmed the effect of FxOH on cell growth in six types of human CRC cells and on CLIC4 expression. We found an inverse association between sensitivity to FxOH in each cell and CLIC4 expression in each control cell. Notably, the sensitivities of DLD-1 and HCT116 cells with higher CLIC4 expression to FxOH were higher than those of LoVo and HT-29 cells with lower CLIC4 expression (Figure 1B-D). However, a minor difference was observed in the microsatellite instability, CpG island methylation phenotype, chromosomal instability pathway, and mutational characteristics among these

Table II. *Down-regulated gene profile in DLD-1 cells with CLIC4 knockdown*[a].

Gene symbol	Description	Fold[b]	*p*-Value[c]
Group 1[d]			
TSC22D3	TSC22 domain family, member 3	–2.45	4.40×10^{-3}
C22orf46	Chromosome 22 open reading frame 46	–2.29	7.17×10^{-5}
TMEM154	Transmembrane protein 154	–2.14	8.00×10^{-4}
LURAP1L	Leucine rich adaptor protein 1-like	–2.07	3.20×10^{-3}
Group 2[e]			
KRTAP3-1	Keratin associated protein 3-1	–8.55	4.56×10^{-9}
ANKRD13C	Ankyrin repeat domain 13C	–7.19	3.41×10^{-9}
JUN	Jun proto-oncogene	–5.22	1.16×10^{-8}
SEMA3C	Sema domain, immunoglobulin domain (Ig), short basic domain, secreted, (semaphorin) 3C	–4.36	6.29×10^{-9}
CACNB3	Calcium channel, voltage-dependent, beta 3 subunit	–3.48	2.61×10^{-7}
PCP4	Purkinje cell protein 4	–3.11	9.07×10^{-5}
TNFRSF19	Tumor necrosis factor receptor superfamily, member 19	–2.86	1.00×10^{-4}
OAS1	2-5-Oligoadenylate synthetase 1	–2.27	3.11×10^{-5}
IFIT2	Interferon-induced protein with tetratricopeptide repeats 2	–2.10	2.30×10^{-5}
Group 3[f]			
CLIC4	Chloride intracellular channel 4	–74.59	1.09×10^{-13}
ARHGEF3	Rho guanine nucleotide exchange factor 3	–14.73	1.52×10^{-9}
SLC39A6	Solute carrier family 39 (zinc transporter), member 6	–12.80	2.94×10^{-11}
NT5E	5-Nucleotidase, ecto (CD73)	–11.66	2.00×10^{-10}
GNG12	Guanine nucleotide binding protein (G protein), gamma 12	–8.23	2.99×10^{-11}
DNAJC22	DnaJ (Hsp40) homolog, subfamily C, member 22	–8.19	8.59×10^{-10}
STAP1	Signal transducing adaptor family member 1	–8.04	2.95×10^{-10}
GBP3	Guanylate binding protein 3	–7.50	4.11×10^{-10}
CYP4V2	Cytochrome P450, family 4, subfamily V, polypeptide 2	–7.01	4.88×10^{-10}
TMEM184C	Transmembrane protein 184C	–6.94	2.52×10^{-9}
PRRG4	Proline rich Gla (G-carboxyglutamic acid) 4 (transmembrane)	–6.77	3.90×10^{-10}
SEPP1	Selenoprotein P, plasma, 1	–6.59	2.91×10^{-8}
PPP1R14C	Protein phosphatase 1, regulatory (inhibitor) subunit 14C	–6.35	4.61×10^{-8}
ZNF652	Zinc finger protein 652	–6.15	8.12×10^{-9}
ROR1	Receptor tyrosine kinase-like orphan receptor 1	–5.99	1.30×10^{-10}
MCOLN3	Mucolipin 3	–5.91	2.35×10^{-8}
HNF4G	Hepatocyte nuclear factor 4, gamma	–5.76	8.03×10^{-9}
SCML1	Sex comb on midleg-like 1 (Drosophila)	–5.71	8.85×10^{-9}
PVRL1	Poliovirus receptor-related 1 (herpesvirus entry mediator C)	–5.67	3.39×10^{-7}
CPNE3	Copine III	–5.65	2.97×10^{-10}
ATP6V1C2	ATPase, H+ transporting, lysosomal 42kDa, V1 subunit C2	–5.64	4.95×10^{-9}
CPOX	Coproporphyrinogen oxidase	–5.59	1.26×10^{-8}
IL17RD	Interleukin 17 receptor D	–5.32	8.63×10^{-9}
KDELR3	KDEL (Lys-Asp-Glu-Leu) endoplasmic reticulum protein retention receptor 3	–5.09	3.93×10^{-6}
ADSS	Adenylosuccinate synthase	–4.97	5.65×10^{-9}
VAMP3	Vesicle associated membrane protein 3	–4.9	1.01×10^{-9}
TEAD2	TEA domain family member 2	–4.85	1.88×10^{-6}
PRR11	Proline rich 11	–4.81	3.67×10^{-8}
MYD88	Myeloid differentiation primary response 88	–4.66	4.70×10^{-9}
INIP	INTS3 and NABP interacting protein	–4.61	5.65×10^{-9}
ACADVL	Acyl-CoA dehydrogenase, very long chain	–4.59	2.52×10^{-8}
MDFIC	MyoD family inhibitor domain containing	–4.57	2.76×10^{-7}
SDHD	Succinate dehydrogenase complex subunit D, integral membrane protein	–4.57	8.67×10^{-9}
PRKACB	Protein kinase, cAMP-dependent, catalytic, beta	–4.54	8.11×10^{-10}
ELK3	ELK3, ETS-domain protein (SRF accessory protein 2)	–4.47	5.44×10^{-7}
CD46	CD46 molecule, complement regulatory protein	–4.45	1.91×10^{-9}
FILIP1L	Filamin A interacting protein 1-like	–4.42	8.14×10^{-7}

Table II. *Continued*

Table II. *Continued*

Gene symbol	Description	Fold[b]	*p*-Value[c]
MOB3C	MOB kinase activator 3C	–4.41	2.76×10^{-7}
SLC39A10	Solute carrier family 39 (zinc transporter), member 10	–4.41	1.13×10^{-6}
MYB	v-Myb avian myeloblastosis viral oncogene homolog	–4.36	1.29×10^{-7}
ZNF559-ZNF177	ZNF559-ZNF177 readthrough	–4.30	3.95×10^{-6}
PTMS	Parathymosin	–4.30	7.73×10^{-8}
UQCRC2	Ubiquinol-cytochrome c reductase core protein II	–4.26	4.77×10^{-10}
BBS1	Bardet-Biedl syndrome 1	–4.22	8.93×10^{-8}
CD84	CD84 molecule	–4.21	3.00×10^{-7}
NIPAL2	NIPA-like domain containing 2	–4.18	3.27×10^{-9}
PCMTD1	Protein-L-isoaspartate (D-aspartate) O-methyltransferase domain containing 1	–4.17	2.11×10^{-6}
PXK	PX domain containing serine/threonine kinase	–4.15	3.71×10^{-9}
AMACR	Alpha-methylacyl-CoA racemase	–4.15	1.49×10^{-9}
KIF20A	Kinesin family member 20A	–4.09	8.19×10^{-8}
CSTL1	Cystatin-like 1	–4.08	1.00×10^{-4}
SOCS2	Suppressor of cytokine signaling 2	–4.08	1.46×10^{-8}

[a]Among all 502 down-regulated genes with significant alterations, the 56 genes with ≤–4.0-fold and 9 genes with >–4.0 and ≤–2.0-fold are shown. [b]Fold change of gene expression in DLD-1 cells with CLIC4 knockdown, compared with that of control cells. [c]Significant differences between DLD-1 cells with and without CLIC4 knockdown using one-way ANOVA (n=3). [d]Group 1, genes down-regulated in both CLIC4 knockdown and overexpression in DLD-1 cells, corresponding to those of group 1 in Table IV. [e]Group 2, genes down-regulated in CLIC4 knockdown and up-regulated in CLIC4 overexpression, corresponding to those of group 2 in Table III. [f]Group 3, genes down-regulated in CLIC4 knockdown but not detected CLIC4 overexpression.

four types of human CRC cells (46). We examined the molecular mechanisms triggered by CLIC4 knockdown and overexpression in DLD-1 cells.

Transcriptome changes based on CLIC4 knockdown and overexpression demonstrated that 15 cancer-related signals, namely, NR, insulin, PI3K/AKT, adhesion, VEGF, MAPK, NRF2, endothelin, IL-18, EMT, TGF-β, interferon, p53, immune response, and miRNA regulation (CLIC4-related signals), were significantly altered in CRC cells compared to the negative control cells (Figure 2A-E, Figure 4A-E and Figure 6A). FxOH treatment (5.0 μmol/l) has been reported to induce apoptosis and anoikis, anchor-dependent cell death, in DLD-1 cells *via* attenuation of integrin signaling (44, 45). In the two previous reports, we displayed 11 cancer-related signals among the top 20 signals altered on the FxOH-treated DLD-1cells (Figure 6B): NR, VEGF, adhesion (containing integrin signals), NRF2, MAPK, PI3K/AKT, insulin, IL-18, microRNA regulation, EGFR, and cell cycle (43). Among these 11 cancer-related signals, 9 signals (82%), *i.e.*, NR, VEGF, adhesion, NRF2, MAPK, PI3K/AKT, insulin, IL-18, and miRNA regulation, were overlapped with the CLIC4-related signals. Thus, CLIC4 is suggested to be a central regulator of apoptosis and anoikis induction by FxOH in DLD-1 cells (Figure 6B).

CLIC4 regulates or is regulated by molecules, such as the G-protein-coupled receptor, Rho A, F-actin, integrin, NHERF2, KRAS, p53, and TNF-α, and signals, such as apoptosis, angiogenesis, cell adhesion, and TGF-β (16-18, 21, 22, 39-42, 47). In the present study, we discovered many novel CLIC4-related molecules and signals affecting the development of cancer cells, other than those described in previous studies (Figure 2A-E, Figure 4A-E, Table I, Table II, Table III, and Table IV). Genes exhibited the opposite expression pattern in DLD-1 cells between CLIC4 knockdown and overexpression; *FERMT2*, *GPR1*, *VLDLR, KRTAP3-1*, *IFIT2*, *OAS1*, *TNFRSF19*, *ANKRD13C*, *PCP4*, *JUN*, *CACNB3* and *SEMA3C* were expected to be involved in growth inhibition by CLIC4 knockdown and in CRC development by CLIC4 overexpression (Table I, Table II, Table III, and Table IV). On the other hand, common cell conditions acquired in DLD-1 cells by both CLIC4

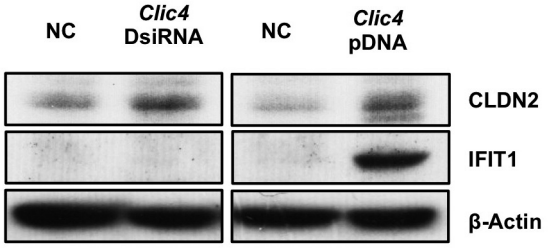

Figure 5. *Protein expression levels in DLD-1 cells with CLIC4 knockdown or overexpression. DLD-1 cells were treated with Clic4 dsiRNA or plasmid DNA [(p)DNA] for 2 days. The CLIC4 protein level was measured by western blotting. NC, negative control.*

Table III. *Up-regulated gene profile in DLD-1 cells with CLIC4 overexpression*[a].

Gene symbol	Description	Fold[b]	*p*-Value[c]
Group 1[d]			
IFIT1	Interferon-induced protein with tetratricopeptide repeats 1	8.34	3.54×10^{-5}
CLDN2	Claudin 2	3.63	0.0001
LIPG	Lipase, endothelial	3.38	1.28×10^{-5}
SLC1A3	Solute carrier family 1, member 3	2.46	4.37×10^{-7}
ERP27	Endoplasmic reticulum protein 27	2.22	6.09×10^{-6}
FGFBP1	Fibroblast growth factor binding protein 1	2.01	0.0004
Group 2[e]			
KRTAP3-1	Keratin associated protein 3-1	7.18	3.68×10^{-7}
IFIT2	Interferon-induced protein with tetratricopeptide repeats 2	4.22	3.81×10^{-10}
OAS1	2-5-Oligoadenylate synthetase 1	2.64	8.50×10^{-5}
TNFRSF19	Tumor necrosis factor receptor superfamily, member 19	2.62	0.0005
ANKRD1	Ankyrin repeat domain 1 (cardiac muscle)	2.44	3.92×10^{-5}
PCP4	Purkinje cell protein 4	2.25	0.0001
JUN	Jun proto-oncogene	2.22	8.80×10^{-5}
CACNB3	Calcium channel, voltage-dependent, beta 3 subunit	2.12	0.0025
SEMA3C	Sema domain, immunoglobulin domain (Ig), short basic domain, secreted, (semaphorin) 3C	2.12	0.0005
Group 3[f]			
IFI6	Interferon, alpha-inducible protein 6	9.37	4.14×10^{-10}
HIST1H2BM	Histone cluster 1, H2bm	3.18	0.0077
DBF4	Transcript Identified by AceView, Entrez Gene ID(s) 10926	2.72	0.0025
BCL2L15	BCL2-like 15	2.67	7.93×10^{-6}
EPN3	Epsin 3	2.44	2.33×10^{-5}
HPGD	Hydroxyprostaglandin dehydrogenase 15-(NAD)	2.32	1.41×10^{-5}
ANKRD22	Ankyrin repeat domain 22	2.23	0.0002
MX2	MX dynamin-like GTPase 2	2.20	5.80×10^{-5}
RELT	RELT tumor necrosis factor receptor	2.17	0.0002
GRHL3	Grainyhead-like transcription factor 3	2.14	2.97×10^{-5}
SLAMF6	SLAM family member 6	2.14	0.0023
OLFML3	Olfactomedin like 3	2.13	7.00×10^{-5}
TNFRSF11A	Transcript Identified by AceView, Entrez Gene ID(s) 8792	2.13	0.0109
GAL	Galanin/GMAP prepropeptide	2.12	0.0007
IFIT3	Interferon-induced protein with tetratricopeptide repeats 3	2.12	0.0002
NMU	Neuromedin U	2.11	0.0003
TGIF2	TGFB-induced factor homeobox 2	2.10	1.34×10^{-5}
EGLN3	Egl-9 family hypoxia-inducible factor 3	2.10	0.0001
KIT	v-Kit Hardy-Zuckerman 4 feline sarcoma viral oncogene homolog	2.09	0.0006
FLOT2	Memczak2013 ANTISENSE, CDS, coding, INTERNAL, intronic best transcript NM_004475	2.08	0.0207
NUDT7	Nudix hydrolase 7	2.07	0.0213
RAB30	RAB30, member RAS oncogene family	2.04	4.76×10^{-6}
ZNF454	Zinc finger protein 454	2.03	0.0483

[a]Among all 69 up-regulated genes with significant alterations, the 38 genes with ≥2.0-fold are shown. [b]Fold change of gene expression in DLD-1 cells with CLIC4 overexpression in comparison with those of the negative control cells. [c]Significant differences between DLD-1 cells with and without CLIC4 overexpression using one-way ANOVA (n=3). [d]Group 1, genes up-regulated in both CLIC4 overexpression and knockdown in DLD-1 cells, corresponding to those of group 1 in Table I. [e]Group 2, genes up-regulated in CLIC4 overexpression and down-regulated in CLIC4 knockdown, corresponding to those of group 2 in Table II. [f]Group 3, genes up-regulated in CLIC4 overexpression but not detected in CLIC4 knockdown.

knockdown and overexpression were the decreased sensitivity to FxOH exposure (Figure 1F and Figure 3B). Therefore, common up-regulated genes, like *CLDN2*, *ERP27*, *IFIT1*, *FGFBP1*, *SLC1A3* and *LIPG*, or common down-regulated genes, including *TSC22D3*, *C22orf46*, *TMEM154* and *LURAP1L*, in the cells by both CLIC4 knockdown and overexpression may be involved in the decreased sensitivity to FxOH (Table I, Table II, Table III, and Table IV). These results were another novel finding. In addition, CLDN2 and IFIT1 protein expression levels

Table IV. *Down-regulated gene profile in DLD-1 cells with CLIC4 overexpression*[a].

Gene symbol	Description	Fold[b]	*p*-Value[c]
Group 1[d]			
TSC22D3	TSC22 domain family, member 3	–2.44	1.92×10^{-6}
C22orf46	Chromosome 22 open reading frame 46	–2.44	0.0006
TMEM154	Transmembrane protein 154	–2.15	8.59×10^{-5}
LURAP1L	Leucine rich adaptor protein 1-like	–2.03	0.0008
Group 2[e]			
GPR1	G protein-coupled receptor 1	–2.48	5.75×10^{-6}
VLDLR	Very low-density lipoprotein receptor	–2.24	0.0003
FERMT2	Fermitin family member 2	–2.06	3.63×10^{-5}
Group 3[f]			
FAM129A	Family with sequence similarity 129, member A	–4.00	2.04×10^{-8}
DDIT4	DNA damage inducible transcript 4	–3.42	1.92×10^{-8}
SESN2	Sestrin 2	–2.66	8.39×10^{-8}
PLEKHG1	Pleckstrin homology domain containing, family G (with RhoGef domain) member 1	–2.46	3.48×10^{-7}
PDE10A	Phosphodiesterase 10A	–2.42	0.0001
TXNIP	Thioredoxin interacting protein	–2.36	1.27×10^{-6}
ULBP1	UL16 binding protein 1	–2.35	4.73×10^{-6}
GTPBP2	GTP binding protein 2	–2.25	1.44×10^{-6}
FEM1C	Jeck2013 ALT_ACCEPTOR, ALT_DONOR, coding, INTERNAL, intronic best transcript NM_020177	–2.21	0.0107
FAM107B	Family with sequence similarity 107, member B	–2.21	5.21×10^{-6}
GTF2A1L	General transcription factor IIA 1-like	–2.20	0.0202
TRIB3	Tribbles pseudokinase 3	–2.18	7.01×10^{-6}
HSPA13	Heat shock protein 70kDa family, member 13	–2.12	8.75×10^{-7}
SLC7A11	Solute carrier family 7 (anionic amino acid transporter light chain, xc- system), member 11	–2.11	3.24×10^{-7}
CHAC1	ChaC glutathione-specific gamma-glutamylcyclotransferase 1	–2.10	6.08×10^{-7}
PDGFA	Platelet-derived growth factor alpha polypeptide	–2.07	4.14×10^{-5}
ZNF479	Zinc finger protein 479	–2.06	0.0066
LCN2	Lipocalin 2	–2.06	0.0005
PLEKHH2	Pleckstrin homology domain containing, family H (with MyTH4 domain) member 2	–2.06	0.0001
HOMER2	Homer scaffolding protein 2	–2.05	0.0036
FAM27E3	Family with sequence similarity 27, member E3	–2.03	1.39×10^{-5}
ARHGEF2	Rho/Rac guanine nucleotide exchange factor 2	–2.03	3.35×10^{-6}
SLC6A9	Solute carrier family 6 (neurotransmitter transporter, glycine), member 9	–2.03	5.64×10^{-6}
PDE9A	Phosphodiesterase 9A	–2.02	0.001

[a]Among all 69 up-regulated genes with significant alterations, the 31 genes with ≤–2.0-fold were shown. [b]Fold change of gene expression in DLD-1 cells with CLIC4 overexpression, compared with that of control cells. [c]Significant differences between DLD-1 cells with and without CLIC4 overexpression using one-way ANOVA (n=3). [d]Group 1, genes down-regulated in both CLIC4 knockdown and overexpression in DLD-1 cells, corresponding to those of group 1 in Table II. [e]Group 2, genes down-regulated in CLIC4 overexpression and up-regulated in CLIC4 knockdown, corresponding to those of group 2 in Table I. [f]Group 3, genes down-regulated in CLIC4 overexpression but not detected in CLIC4 knockdown.

increased in DLD-1 cells following CLIC4 knockdown and/or overexpression (Figure 5). CLDN2 is a tight junction modulator that is involved in cancer proliferation, migration, and metastasis. CLDN2 expression contributes to chemoresistance in CRC cells and is associated with poor outcomes in patients with CRC (48, 49). ERP27 is an endoplasmic reticulum protein, and the gene is highly expressed in patients with CRC (50). IFIT1 is an interferon-stimulated inflammation-related protein that promotes cell invasion, metastasis, and tumor development (51). FGFBP1 releases fibroblast growth factors-interacting fibroblast growth factor receptors from extracellular matrix and enhances the migration and invasion of cancer cells (52). SLC1A3 is a glutamate/aspartate transporter that promotes

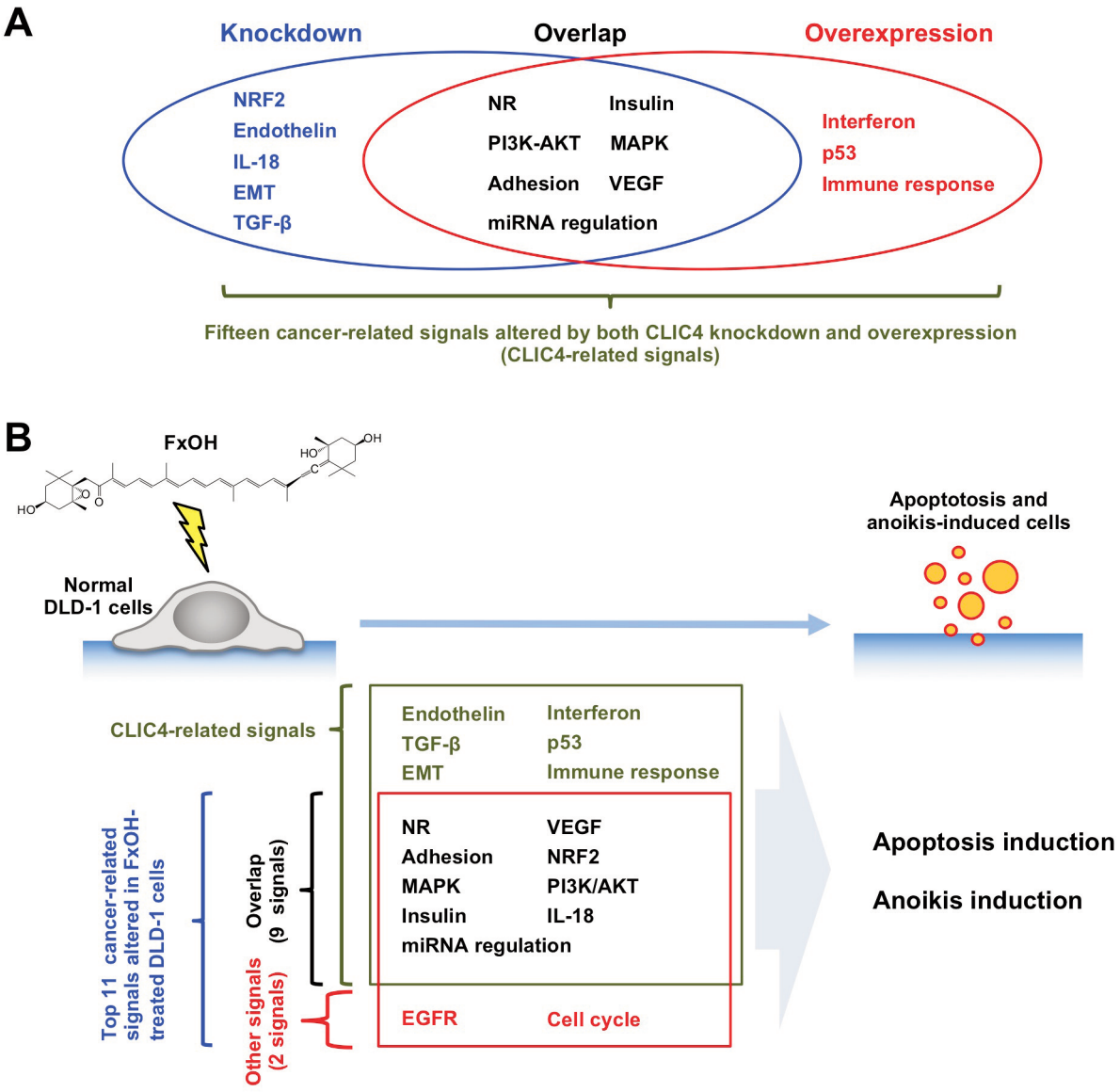

Figure 6. *Possible mechanisms underlying DLD-1 cells with CLIC4 alteration by FxOH treatment. (A) Venn diagram of signals changed in DLD-1 cells with CLIC4 knockdown and overexpression. Blue and red correspond to signals altered in CLIC4 knockdown and overexpressing DLD-1 cells, respectively. Black, signals altered in both CLIC4 knockdown and overexpressing DLD-1 cells. These 15 signals were represented as 15 cancer-related signals altered by both CLIC4 knockdown and overexpression (CLIC4-related signals). (B) Nine of CLIC4-related signals, NR, VEGF, adhesion, NRF2, MAPK, PI3K/AKT, insulin, IL-18, and miRNA regulation among the 15 of CLIC4-related signals, were overlapped with the top 11 cancer-related signals, NR, VEGF, adhesion, NRF2, MAPK, PI3K/AKT, insulin, IL-18, miRNA regulation, EGFR, and cell cycle, altered in FxOH-treated DLD-1 cells, which were represented based on previous reports (38, 43, 44). EGFR and cell cycle among 11 cancer-related signals were represented as other signals without overlap to CLIC4-related signals. The overlay of each signal group suggests that the CLIC4-related signals play significant role for apoptosis and anoikis inductions in FxOH-treated DLD-1 cells.*

tumor metabolism and progression *via* activation of the PI3K/AKT signal (53). LIPG, a protein exhibiting lipase activity, plays a significant role in plasma high-density lipoprotein metabolism and augments tumor formation and metastasis (54). However, the functions of TSC22D3, C22orf46, TMEM154, and LURAP1L in cancer cells remain unclear. Little is known about the associations among CLIC4 and CLDN2, ERP27, IFIT1, FGFBP1, SLC1A3, LIPG, TSC22D3, C22orf46, TMEM154, or LURAP1L.

Several studies have demonstrated the effects of CLIC4 knockdown or overexpression in various cancer cells. CLIC4 knockdown can attenuate cell-matrix adhesion, cellular

spreading, and integrin signals in human cervical cancer (HeLa) and breast cancer (MDA-MB-231) cells, while enhancing their cell motility (16). Thus, there is a case in which CLIC4 knockdown not only unilaterally weakens the development of cancer cells but also leads to the induction of an alternative signal related to development. In addition, photodynamic therapy (PDT) suppresses the invasion ability with the decrease in CLIC4 and metalloproteinase 9 (MMP9) expression levels in human A375 melanoma and MDA-MB-231 cells, but CLIC4 overexpression enhances the invasion ability and attenuates PDT-induced suppressive effect on the invasion abilities of both cells (55). These two prior findings led us to speculate that induction of complete cell death in cancer cells targeting CLIC4 expression using a combination of FxOH and a CLIC4 expression-altering agents may be difficult.

In summary, an inverse association between the FxOH sensitivities in six types of human CRC cells and the protein expression level of CLIC4 in each control cell was found. In addition, CLIC4 knockdown and overexpression suggested that CLIC4 was involved in 11 signals among the top 20 cancer-associated signals altered by apoptosis and anoikis induction in DLD-1 cells by FxOH treatment. Interestingly, both CLIC4 knockdown and overexpression attenuated the FxOH-induced growth inhibition in DLD-1 cells by FxOH treatment. CLDN2, ERP27, IFIT1, FGFBP1, SLC1A3, LIPG, TSC22D3, C22orf46, TMEM154, and LURAP1L induced by CLIC4 alteration may be key molecules responsible for the decreased sensitivity of these cells. These results suggest that CLIC4 must be specifically traced for cell death in human CRC cells by FxOH treatment. Further studies are needed to elucidate the contribution of CLIC4 to the effects of Fx and FxOH in CRC.

Conflicts of Interest

None declared.

Authors' Contributions

R. Y. and M. T. conceived, designed the study, and wrote the paper. R.Y., A. K., S. Y., T. O., and M. T performed the experiments. A. K., H. K., J. H., and H. M. reviewed and edited the manuscript.

Acknowledgements

This work was supported in part by the Japan Society for the Promotion of Science KAKENHI (no. 20K05879).

References

1 Sung H, Ferlay J, Siegel RL, Laversanne M, Soerjomataram I, Jemal A and Bray F: Global Cancer Statistics 2020: GLOBOCAN estimates of incidence and mortality worldwide for 36 cancers in 185 countries. CA Cancer J Clin *71(3)*: 209-249, 2021. PMID: 33538338. DOI: 10.3322/caac.21660

2 Arnold M, Sierra MS, Laversanne M, Soerjomataram I, Jemal A and Bray F: Global patterns and trends in colorectal cancer incidence and mortality. Gut *66(4)*: 683-691, 2017. PMID: 26818619. DOI: 10.1136/gutjnl-2015-310912

3 Pearlman R, Frankel WL, Swanson B, Zhao W, Yilmaz A, Miller K, Bacher J, Bigley C, Nelsen L, Goodfellow PJ, Goldberg RM, Paskett E, Shields PG, Freudenheim JL, Stanich PP, Lattimer I, Arnold M, Liyanarachchi S, Kalady M, Heald B, Greenwood C, Paquette I, Prues M, Draper DJ, Lindeman C, Kuebler JP, Reynolds K, Brell JM, Shaper AA, Mahesh S, Buie N, Weeman K, Shine K, Haut M, Edwards J, Bastola S, Wickham K, Khanduja KS, Zacks R, Pritchard CC, Shirts BH, Jacobson A, Allen B, de la Chapelle A, Hampel H and Ohio Colorectal Cancer Prevention Initiative Study Group: Prevalence and spectrum of germline cancer susceptibility gene mutations among patients with early-onset colorectal cancer. JAMA Oncol *3(4)*: 464-471, 2017. PMID: 27978560. DOI: 10.1001/jamaoncol.2016.5194

4 Cancer Genome Atlas Network: Comprehensive molecular characterization of human colon and rectal cancer. Nature *487(7407)*: 330-337, 2012. PMID: 22810696. DOI: 10.1038/nature11252

5 Fearon ER: Molecular genetics of colorectal cancer. Annu Rev Pathol *6*: 479-507, 2011. PMID: 21090969. DOI: 10.1146/annurev-pathol-011110-130235

6 Yuan W, Li X, Liu L, Wei C, Sun D, Peng S and Jiang L: Comprehensive analysis of lncRNA-associated ceRNA network in colorectal cancer. Biochem Biophys Res Commun *508(2)*: 374-379, 2019. PMID: 30503344. DOI: 10.1016/j.bbrc.2018.11.151

7 Wu Y, Wang X, Wu F, Huang R, Xue F, Liang G, Tao M, Cai P and Huang Y: Transcriptome profiling of the cancer, adjacent non-tumor and distant normal tissues from a colorectal cancer patient by deep sequencing. PLoS One *7(8)*: e41001, 2012. PMID: 22905095. DOI: 10.1371/journal.pone.0041001

8 Legitimo A, Consolini R, Failli A, Orsini G and Spisni R: Dendritic cell defects in the colorectal cancer. Hum Vaccin Immunother *10(11)*: 3224-3235, 2014. PMID: 25483675. DOI: 10.4161/hv.29857

9 Mariani F, Sena P and Roncucci L: Inflammatory pathways in the early steps of colorectal cancer development. World J Gastroenterol *20(29)*: 9716-9731, 2014. PMID: 25110410. DOI: 10.3748/wjg.v20.i29.9716

10 Medema JP and Vermeulen L: Microenvironmental regulation of stem cells in intestinal homeostasis and cancer. Nature *474(7351)*: 318-326, 2011. PMID: 21677748. DOI: 10.1038/nature10212

11 Fehlker M, Huska MR, Jöns T, Andrade-Navarro MA and Kemmner W: Concerted down-regulation of immune-system related genes predicts metastasis in colorectal carcinoma. BMC Cancer *14*: 64, 2014. PMID: 24495478. DOI: 10.1186/1471-2407-14-64

12 O'Keefe SJ: Diet, microorganisms and their metabolites, and colon cancer. Nat Rev Gastroenterol Hepatol *13(12)*: 691-706, 2016. PMID: 27848961. DOI: 10.1038/nrgastro.2016.165

13 Cooks T, Pateras IS, Tarcic O, Solomon H, Schetter AJ, Wilder S, Lozano G, Pikarsky E, Forshew T, Rosenfeld N, Harpaz N, Itzkowitz S, Harris CC, Rotter V, Gorgoulis VG and Oren M: Mutant p53 prolongs NF-κB activation and promotes chronic inflammation and inflammation-associated colorectal cancer. Cancer Cell *23(5)*: 634-646, 2013. PMID: 23680148. DOI: 10.1016/j.ccr.2013.03.022

14 Champeris Tsaniras S, Villiou M, Giannou AD, Nikou S, Petropoulos M, Pateras IS, Tserou P, Karousi F, Lalioti ME, Gorgoulis VG, Patmanidi AL, Stathopoulos GT, Bravou V, Lygerou Z and Taraviras S: Geminin ablation *in vivo* enhances tumorigenesis through increased genomic instability. J Pathol *246(2)*: 134-140, 2018. PMID: 29952003. DOI: 10.1002/path.5128

15 Littler DR, Harrop SJ, Goodchild SC, Phang JM, Mynott AV, Jiang L, Valenzuela SM, Mazzanti M, Brown LJ, Breit SN and Curmi PM: The enigma of the CLIC proteins: Ion channels, redox proteins, enzymes, scaffolding proteins? FEBS Lett *584(10)*: 2093-2101, 2010. PMID: 20085760. DOI: 10.1016/j.febslet.2010.01.027

16 Argenzio E, Margadant C, Leyton-Puig D, Janssen H, Jalink K, Sonnenberg A and Moolenaar WH: CLIC4 regulates cell adhesion and β1 integrin trafficking. J Cell Sci *127(Pt 24)*: 5189-5203, 2014. PMID: 25344254. DOI: 10.1242/jcs.150623

17 Suh KS, Mutoh M, Nagashima K, Fernandez-Salas E, Edwards LE, Hayes DD, Crutchley JM, Marin KG, Dumont RA, Levy JM, Cheng C, Garfield S and Yuspa SH: The organellular chloride channel protein CLIC4/mtCLIC translocates to the nucleus in response to cellular stress and accelerates apoptosis. J Biol Chem *279(6)*: 4632-4641, 2004. PMID: 14610078. DOI: 10.1074/jbc.M311632200

18 Ulmasov B, Bruno J, Gordon N, Hartnett ME and Edwards JC: Chloride intracellular channel protein-4 functions in angiogenesis by supporting acidification of vacuoles along the intracellular tubulogenic pathway. Am J Pathol *174(3)*: 1084-1096, 2009. PMID: 19197003. DOI: 10.2353/ajpath.2009.080625

19 Padmakumar VC, Speer K, Pal-Ghosh S, Masiuk KE, Ryscavage A, Dengler SL, Hwang S, Edwards JC, Coppola V, Tessarollo L, Stepp MA and Yuspa SH: Spontaneous skin erosions and reduced skin and corneal wound healing characterize CLIC4(NULL) mice. Am J Pathol *181(1)*: 74-84, 2012. PMID: 22613027. DOI: 10.1016/j.ajpath.2012.03.025

20 Zou L, Chen W, Zhou X, Yang T, Luo J, Long Z, Wu J, Lv D, Mao×and Cen S: N6-methyladenosine demethylase FTO suppressed prostate cancer progression by maintaining CLIC4 mRNA stability. Cell Death Discov *8(1)*: 184, 2022. PMID: 35397614. DOI: 10.1038/s41420-022-01003-7

21 Okudela K, Katayama A, Woo T, Mitsui H, Suzuki T, Tateishi Y, Umeda S, Tajiri M, Masuda M, Nagahara N, Kitamura H and Ohashi K: Proteome analysis for downstream targets of oncogenic KRAS – the potential participation of CLIC4 in carcinogenesis in the lung. PLoS One *9(2)*: e87193, 2014. PMID: 24503901. DOI: 10.1371/journal.pone.0087193

22 Fernández-Salas E, Sagar M, Cheng C, Yuspa SH and Weinberg WC: p53 and tumor necrosis factor alpha regulate the expression of a mitochondrial chloride channel protein. J Biol Chem *274(51)*: 36488-36497, 1999. PMID: 10593946. DOI: 10.1074/jbc.274.51.36488

23 Yokoyama R, Kubota A, Kojima H, Tanaka T, Mutoh M and Terasaki M: Detection of cells displaying high expression of CLIC4 in tumor tissue of patients with colorectal cancer. In Vivo *35(6)*: 3165-3173, 2021. PMID: 34697147. DOI: 10.21873/invivo.12611

24 Suh KS, Crutchley JM, Koochek A, Ryscavage A, Bhat K, Tanaka T, Oshima A, Fitzgerald P and Yuspa SH: Reciprocal modifications of CLIC4 in tumor epithelium and stroma mark malignant progression of multiple human cancers. Clin Cancer Res *13(1)*: 121-131, 2007. PMID: 17200346. DOI: 10.1158/1078-0432.CCR-06-1562

25 Deng YJ, Tang N, Liu C, Zhang JY, An SL, Peng YL, Ma LL, Li GQ, Jiang Q, Hu CT, Wang YN, Liang YZ, Bian XW, Fang WG and Ding YQ: CLIC4, ERp29, and Smac/DIABLO derived from metastatic cancer stem-like cells stratify prognostic risks of colorectal cancer. Clin Cancer Res *20(14)*: 3809-3817, 2014. PMID: 24916695. DOI: 10.1158/1078-0432.CCR-13-1887

26 Mikami K and Hosokawa M: Biosynthetic pathway and health benefits of fucoxanthin, an algae-specific xanthophyll in brown seaweeds. Int J Mol Sci *14(7)*: 13763-13781, 2013. PMID: 23820585. DOI: 10.3390/ijms140713763

27 Spagolla Napoleão Tavares R, Maria-Engler SS, Colepicolo P, Debonsi HM, Schäfer-Korting M, Marx U, Gaspar LR and Zoschke C: Skin irritation testing beyond tissue viability: fucoxanthin effects on inflammation, homeostasis, and metabolism. Pharmaceutics *12(2)*: 136, 2020. PMID: 32033492. DOI: 10.3390/pharmaceutics12020136

28 Iio K, Okada Y and Ishikura M: [Single and 13-week oral toxicity study of fucoxanthin oil from microalgae in rats]. Shokuhin Eiseigaku Zasshi *52(3)*: 183-189, 2011. PMID: 21720124. DOI: 10.3358/shokueishi.52.183

29 Beppu F, Niwano Y, Tsukui T, Hosokawa M and Miyashita K: Single and repeated oral dose toxicity study of fucoxanthin (FX), a marine carotenoid, in mice. J Toxicol Sci *34(5)*: 501-510, 2009. PMID: 19797858. DOI: 10.2131/jts.34.501

30 Asai A, Yonekura L and Nagao A: Low bioavailability of dietary epoxyxanthophylls in humans. Br J Nutr *100(2)*: 273-277, 2008. PMID: 18186952. DOI: 10.1017/S0007114507895468

31 Hashimoto T, Ozaki Y, Mizuno M, Yoshida M, Nishitani Y, Azuma T, Komoto A, Maoka T, Tanino Y and Kanazawa K: Pharmacokinetics of fucoxanthinol in human plasma after the oral administration of kombu extract. Br J Nutr *107(11)*: 1566-1569, 2012. PMID: 21920061. DOI: 10.1017/S0007114511004879

32 Yonekura L, Kobayashi M, Terasaki M and Nagao A: Keto-carotenoids are the major metabolites of dietary lutein and fucoxanthin in mouse tissues. J Nutr *140(10)*: 1824-1831, 2010. PMID: 20739451. DOI: 10.3945/jn.110.126466

33 Terasaki M, Kubota A, Kojima H, Maeda H, Miyashita K, Kawagoe C, Mutoh M and Tanaka T: Fucoxanthin and colorectal cancer prevention. Cancers (Basel) *13(10)*: 2379, 2021. PMID: 34069132. DOI: 10.3390/cancers13102379

34 Terasaki M, Ono S, Hashimoto S, Kubota A, Kojima H, Ohta T, Tanaka T, Maeda H, Miyashita K and Mutoh M: Suppression of C-C chemokine receptor 1 is a key regulation for colon cancer chemoprevention in AOM/DSS mice by fucoxanthin. J Nutr Biochem *99*: 108871, 2022. PMID: 34571188. DOI: 10.1016/j.jnutbio.2021.108871

35 Murase W, Kamakura Y, Kawakami S, Yasuda A, Wagatsuma M, Kubota A, Kojima H, Ohta T, Takahashi M, Mutoh M, Tanaka T, Maeda H, Miyashita K and Terasaki M: Fucoxanthin prevents pancreatic tumorigenesis in C57BL/6J mice that received allogenic and orthotopic transplants of cancer cells. Int J Mol Sci *22(24)*: 13620, 2021. PMID: 34948416. DOI: 10.3390/ijms222413620

36 Terasaki M, Inoue T, Murase W, Kubota A, Kojima H, Kojoma M, Ohta T, Maeda H, Miyashita K, Mutoh M and Takahashi M: A Fucoxanthinol induces apoptosis in a pancreatic intraepithelial neoplasia cell. Cancer Genomics Proteomics *18(2)*: 133-146, 2021. PMID: 33608310. DOI: 10.21873/cgp.20248

37 Terasaki M, Nishizaka Y, Murase W, Kubota A, Kojima H, Kojoma M, Tanaka T, Maeda H, Miyashita K, Mutoh M and Takahashi M: Effect of fucoxanthinol on pancreatic ductal

adenocarcinoma cells from an *N*-Nitrosobis(2-oxopropyl)amine-initiated Syrian golden hamster pancreatic carcinogenesis model. Cancer Genomics Proteomics *18(3 Suppl)*: 407-423, 2021. PMID: 33994364. DOI: 10.21873/cgp.20268

38 Yokoyama R, Kojima H, Takai R, Ohta T, Maeda H, Miyashita K, Mutoh M and Terasaki M: Effects of CLIC4 on fucoxanthinol-induced apoptosis in human colorectal cancer cells. Nutr Cancer *73(5)*: 889-898, 2021. PMID: 33703973. DOI: 10.1080/01635581.2020.1779760

39 Alday-Parejo B, Stupp R and Rüegg C: Are integrins still practicable targets for anti-cancer therapy? Cancers (Basel) *11(7)*: 978, 2019. PMID: 31336983. DOI: 10.3390/cancers11070978

40 Yoshida M, Zhao L, Grigoryan G, Shim H, He P and Yun CC: Deletion of Na+/H+ exchanger regulatory factor 2 represses colon cancer progress by suppression of Stat3 and CD24. Am J Physiol Gastrointest Liver Physiol *310(8)*: G586-G598, 2016. PMID: 26867566. DOI: 10.1152/ajpgi.00419.2015

41 Pietenpol JA, Holt JT, Stein RW and Moses HL: Transforming growth factor beta 1 suppression of c-myc gene transcription: role in inhibition of keratinocyte proliferation. Proc Natl Acad Sci USA *87(10)*: 3758-3762, 1990. PMID: 2187192. DOI: 10.1073/pnas.87.10.3758

42 Massagué J, Blain SW and Lo RS: TGFbeta signaling in growth control, cancer, and heritable disorders. Cell *103(2)*: 295-309, 2000. PMID: 11057902. DOI: 10.1016/s0092-8674(00)00121-5

43 Terasaki M, Takahashi S, Nishimura R, Kubota A, Kojima H, Ohta T, Hamada J, Kuramitsu Y, Maeda H, Miyashita K, Takahashi M and Mutoh M: A marine carotenoid of fucoxanthinol accelerates the growth of human pancreatic cancer PANC-1 cells. Nutr Cancer *74(1)*: 357-371, 2022. PMID: 33590779. DOI: 10.1080/01635581.2020.1863994

44 Terasaki M, Maeda H, Miyashita K and Mutoh M: Induction of anoikis in human colorectal cancer cells by fucoxanthinol. Nutr Cancer *69(7)*: 1043-1052, 2017. PMID: 28990814. DOI: 10.1080/01635581.2017.1339814

45 Terasaki M, Iida T, Kikuchi F, Tamura K, Endo T, Kuramitsu Y, Tanaka T, Maeda H, Miyashita K and Mutoh M: Fucoxanthin potentiates anoikis in colon mucosa and prevents carcinogenesis in AOM/DSS model mice. J Nutr Biochem *64*: 198-205, 2019. PMID: 30530259. DOI: 10.1016/j.jnutbio.2018.10.007

46 Ahmed D, Eide PW, Eilertsen IA, Danielsen SA, Eknæs M, Hektoen M, Lind GE and Lothe RA: Epigenetic and genetic features of 24 colon cancer cell lines. Oncogenesis *2*: e71, 2013. PMID: 24042735. DOI: 10.1038/oncsis.2013.35

47 Ponsioen B, van Zeijl L, Langeslag M, Berryman M, Littler D, Jalink K and Moolenaar WH: Spatiotemporal regulation of chloride intracellular channel protein CLIC4 by RhoA. Mol Biol Cell *20(22)*: 4664-4672, 2009. PMID: 19776349. DOI: 10.1091/mbc.e09-06-0529

48 Paquet-Fifield S, Koh SL, Cheng L, Beyit LM, Shembrey C, Mølck C, Behrenbruch C, Papin M, Gironella M, Guelfi S, Nasr R, Grillet F, Prudhomme M, Bourgaux JF, Castells A, Pascussi JM, Heriot AG, Puisieux A, Davis MJ, Pannequin J, Hill AF, Sloan EK and Hollande F: Tight junction protein claudin-2 promotes self-renewal of human colorectal cancer stem-like cells. Cancer Res *78(11)*: 2925-2938, 2018. PMID: 29510994. DOI: 10.1158/0008-5472.CAN-17-1869

49 Mezheyeuski A, Strell C, Hrynchyk I, Guren TK, Dragomir A, Doroshenko T, Pashkova O, Gorgun J, Ruksha K, Pfeiffer P, Kure EH, Sorbye H, Edler D, Martling A, Glimelius B, Östman A and Portyanko A: Treatment-related survival associations of claudin-2 expression in fibroblasts of colorectal cancer. Virchows Arch *472(3)*: 395-405, 2018. PMID: 29134439. DOI: 10.1007/s00428-017-2263-3

50 Yu Y, Werdyani S, Carey M, Parfrey P, Yilmaz YE and Savas S: A comprehensive analysis of SNPs and CNVs identifies novel markers associated with disease outcomes in colorectal cancer. Mol Oncol *15(12)*: 3329-3347, 2021. PMID: 34309201. DOI: 10.1002/1878-0261.13067

51 Pidugu VK, Wu MM, Yen AH, Pidugu HB, Chang KW, Liu CJ and Lee TC: IFIT1 and IFIT3 promote oral squamous cell carcinoma metastasis and contribute to the anti-tumor effect of gefitinib *via* enhancing p-EGFR recycling. Oncogene *38(17)*: 3232-3247, 2019. PMID: 30626937. DOI: 10.1038/s41388-018-0662-9

52 Zhang Z, Qin Y, Ji S, Xu W, Liu M, Hu Q, Ye Z, Fan G, Yu X, Liu W and Xu X: FGFBP1-mediated crosstalk between fibroblasts and pancreatic cancer cells *via* FGF22/FGFR2 promotes invasion and metastasis of pancreatic cancer. Acta Biochim Biophys Sin (Shanghai) *53(8)*: 997-1008, 2021. PMID: 34117747. DOI: 10.1093/abbs/gmab074

53 Xu L, Chen J, Jia L, Chen X, Awaleh Moumin F and Cai J: SLC1A3 promotes gastric cancer progression *via* the PI3K/AKT signalling pathway. J Cell Mol Med *24(24)*: 14392-14404, 2020. PMID: 33145952. DOI: 10.1111/jcmm.16060

54 Lo PK, Yao Y and Zhou Q: Inhibition of LIPG phospholipase activity suppresses tumor formation of human basal-like triple-negative breast cancer. Sci Rep *10(1)*: 8911, 2020. PMID: 32488004. DOI: 10.1038/s41598-020-65400-7

55 Chiang PC, Chou RH, Chien HF, Tsai T and Chen CT: Chloride intracellular channel 4 involves in the reduced invasiveness of cancer cells treated by photodynamic therapy. Lasers Surg Med *45(1)*: 38-47, 2013. PMID: 23322262. DOI: 10.1002/lsm.22112

Received March 30, 2022
Revised April 24, 2022
Accepted April 26, 2022